



Universiteit
Leiden
The Netherlands

Sex-specific associations in multiparametric 3 T MRI measurements in adult livers

Liu, C.Y.; Noda, C.; Geest, R.J. van der; Triaire, B.; Kassai, Y.; Bluemke, D.A.; Lima, J.A.C.

Citation

Liu, C. Y., Noda, C., Geest, R. J. van der, Triaire, B., Kassai, Y., Bluemke, D. A., & Lima, J. A. C. (2023). Sex-specific associations in multiparametric 3 T MRI measurements in adult livers. *Abdominal Radiology*, 48(10), 3072-3078. doi:10.1007/s00261-023-03981-3

Version: Publisher's Version

License: [Creative Commons CC BY 4.0 license](https://creativecommons.org/licenses/by/4.0/)

Downloaded from: <https://hdl.handle.net/1887/3754558>

Note: To cite this publication please use the final published version (if applicable).



Sex-specific associations in multiparametric 3 T MRI measurements in adult livers

Chia-Ying Liu¹ · Chikara Noda² · Rob J van der Geest³ · Bruno Triaire¹ · Yoshimori Kassai¹ · David A. Bluemke⁴ · João A. C. Lima²

Received: 20 April 2023 / Revised: 1 June 2023 / Accepted: 5 June 2023 / Published online: 28 June 2023
© The Author(s), under exclusive licence to Springer Science+Business Media, LLC, part of Springer Nature 2023

Abstract

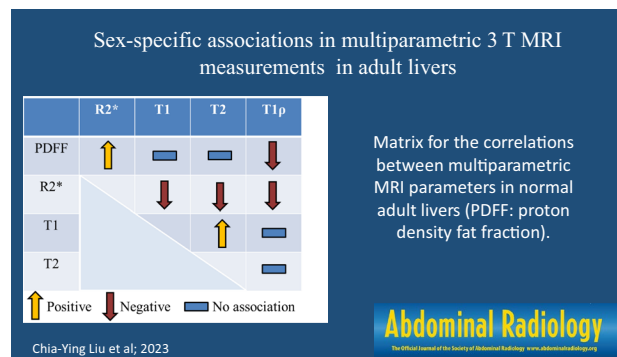
Background MRI relaxometry mapping and proton density fat fraction (PDFF) have been proposed for the evaluation of hepatic fibrosis. However, sex-specific relationships of age and body fat with these MRI parameters have not been studied in detail among adults without clinically manifest hepatic disease. We aimed to determine the sex-specific correlation of multiparametric MRI parameters with age and body fat and to evaluate their interplay associations.

Methods 147 study participants (84 women, mean age 48 ± 14 years, range 19–85 years) were prospectively enrolled. 3 T MRI including T1, T2 and T1 ρ mapping and PDFF and R2* map were acquired. Visceral and subcutaneous fat were measured on the fat images from Dixon water-fat separation sequence.

Results All MRI parameters demonstrated sex difference except for T1 ρ . PDFF was more related to visceral than subcutaneous fat. Per 100 ml gain of visceral or subcutaneous fat is associated with 1 or 0.4% accretion of liver fat, respectively. PDFF and R2* were higher in men (both $P = 0.01$) while T1 and T2 were higher in women (both $P < 0.01$). R2* was positively but T1 and T2 were negatively associated with age in women (all $P < 0.01$), while T1 ρ was positively related to age in men ($P < 0.05$). In all studies, R2* was positively and T1 ρ was negatively associated with PDFF (both $P < 0.0001$).

Conclusion Visceral fat plays an essential role in the elevated liver fat. When using MRI parametric measures for liver disease evaluation, the interplay between these parameters should be considered.

Graphical abstract



Keywords Liver PDFF · T1 · T2 · T1rho · Parametric mapping

Introduction

Imaging biomarkers derived from multiparametric magnetic resonance imaging (MRI) have been investigated for the evaluation of diffuse liver disease [1]. Multiparametric MRI

Extended author information available on the last page of the article

entails the combined use of multiple quantitative images including relaxometry (T1, T2, R2*, and T1 ρ) maps, proton density fat fraction (PDFF), diffusion weighted, susceptibility weighted, dynamic contrast enhanced, spectroscopy, in addition to other techniques to assess specific characteristics of liver disease. Unlike transient elastography with subpar performance in overweight and obese patients [2], MRI is more effective in patients with large body habitus, frequently affected or at risk for hepatic pathologies.

Quantitative MRI maps tissue-specific MR physical properties to provide indices of microstructure and related pathological processes in a time-efficient manner. Hepatic fibrosis and inflammation result in higher T1, T2, and T1 ρ relaxation times due to an excessive accumulation of extracellular matrix proteins and water. Although multiparametric MRI has shown to be useful in evaluating disease severity [3], significant gray zones with wide overlap across severity grades in MRI-derived parametric mapping restrict its clinical relevance [4]. In particular, the coexistence of fat and iron deposition in hepatic tissue confounds the measured relaxation times [5–7]. The relationships between fat and relaxometry parameters have not been fully investigated in individuals with normal livers.

The aim of the present study was twofold. First, we determined the sex-specific correlations of MRI parameters with age, body mass index (BMI), visceral fat, and subcutaneous fat, and then evaluated the interplay among hepatic multiparametric mapping parameters including T1, T2, R2*, and T1 ρ and PDFF measurements in the adult human livers free from liver fibrosis and clinically manifest hepatic disease.

Materials and methods

Our institutional human research ethics committee approved this prospective study and all participants provided written informed consent. Participants were recruited from the local community. There were no specific inclusion criteria except age \geq 18 years, no history of clinical liver disease, and no contraindications to MRI.

MRI was performed using a single 3 T whole-body MRI system (Vantage Galan, Canon Medical Systems, Japan) and a flexible phased array body coil with breath hold. Subcutaneous and visceral fat volumes were measured from three transverse slices of the body at the L2–L3 level by semi-automated segmentation of axial fat images acquired by a two-point Dixon fat-water separation sequence. Hepatic PDFF was assessed using chemical shift-encoded 3D gradient echo (GRE) imaging for joint R2* and fat/water quantification. The sequence included six echoes with 1-ms inter-echo spacing (TR/TE = 7.3/1.2, 2.2, 3.2, 4.3, 5.2, 6.2 ms, flip angle (FA) = 3°) and the post processing incorporated six fat peaks for fat signal determination. A stack of 20 slices

was acquired with a slice thickness of 10 mm and in-plane resolution of 2x2 mm². Inline PDFF and R2* maps were constructed at the scanner using the manufacturer-supplied software. T1 mapping was acquired using a GRE based modified Look-Locker inversion recovery (MOLLI) 5(3)3 with TR/TE = 5.3/1.8 ms, FA = 15° to minimize the influence of fat [5]. T2 mapping was performed using a T2-prepared GRE sequence with TR/TE = 4.5/2 ms, FA = 13°. A rotary echo spin-lock pulse was implemented in a 2D balanced steady-state free precession sequence (TR/TE = 3/1.5 ms, FA = 40°) for the acquisition of T1 ρ maps with a spin-lock frequency of 500 Hz at spinlock times of 1, 15, 30, and 45 ms. All mapping sequences (i.e., T1, T2, and T1 ρ) were acquired at the same level in a single transverse plane with the same slice thickness and in-plane resolution as the PDFF measurements. T1, T2, and T1 ρ maps were constructed offline by using MASS research software (Department of Radiology, Leiden University Medical Center, Leiden, The Netherlands).

Statistical analysis

Liver PDFF, R2*, and parametric mapping indices were determined by averaging the signal within 2–3 cm² ROIs in the corresponding liver parenchyma of all reconstructed mapping images. The ROIs were drawn from areas with minimal signal heterogeneity and while avoiding major vessels. Continuous variables were expressed as mean \pm standard deviation (SD). Sex specific difference was tested using a Mann-Whitney U-test. Sex-specific linear regression was used to investigate the magnitude of associations of age, BMI, visceral, and subcutaneous fat with each MRI parameter. To evaluate which body fat was more correlated to the liver fat, linear regression with visceral and subcutaneous fat co-adjusted was employed. Multivariable analyses adjusted for age, sex and BMI was performed to examine the inter-relationships among the different MRI measures. Statistical evaluations of the data were performed in STATA (Version IC16, StataCorp, College Station, Texas, USA). Adjusted beta was reported and $P < 0.05$ was used for statistical significance.

Results

One hundred and forty-seven adult participants free from clinical liver disease were included in the study (84 women, age range 19 to 85 years). MRI measurements were feasible in all volunteers. Examples of hepatic parametric maps from one of the study participants are shown in Figure 1. Summary statistics stratified by sex are displayed in Table 1. Men and women had similar BMI but body fat was distributed differently with more visceral fat in men and more

Fig. 1 Representative liver magnetic resonance parametric maps at 3 T from a study participant. **a** proton density fat fraction, **b** T1, **c** T2, **d** T1 ρ

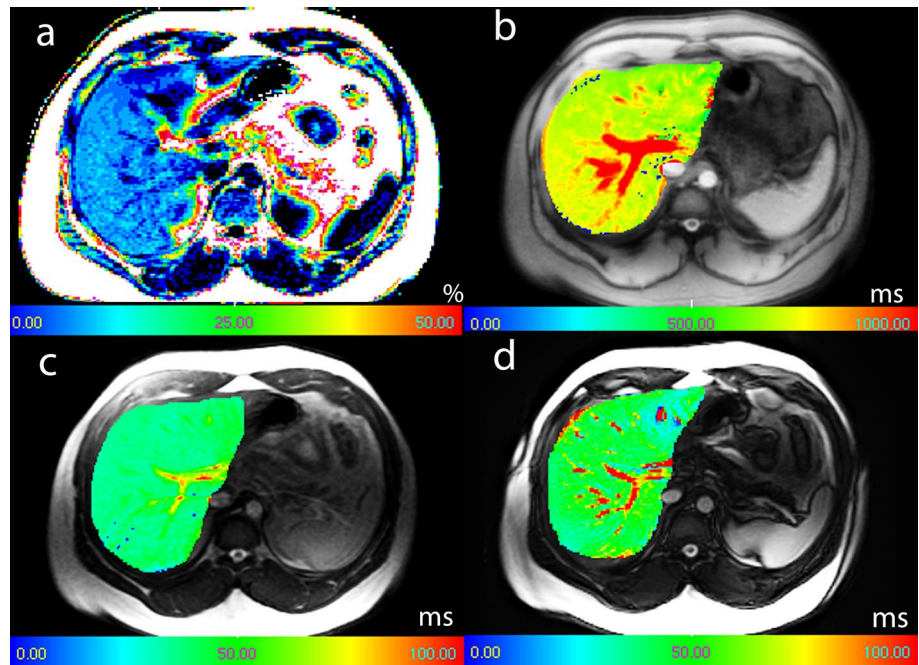


Table 1 Summary of study cohort and multiparametric parameters

<i>N</i>	All	Women	Men	<i>P</i>
	147	84	63	
Age (years)	48 ± 14 (19–85)	47 ± 13 (19–76)	50 ± 16 (19–85)	0.3
BMI (kg/m ²)	28 ± 5 (18–45)	27 ± 6 (18–45)	28 ± 4 (19–39)	0.4
Visceral fat (ml)	461 ± 218 (100–1237)	372 ± 159 (125–770)	580 ± 231 (100–1237)	<0.0001
Subcutaneous fat (ml)	597 ± 289 (199–1738)	672 ± 320 (199–1738)	496 ± 204 (200–1430)	0.0001
PDFF (%)	5.8 ± 5.2 (1.3–28)	5 ± 4.5 (1.3–25)	6.8 ± 6.4 (1.7–28)	0.01
R2* (s ⁻¹)	48 ± 12 (30–85)	45 ± 10 (30–81)	51 ± 13 (32–85)	0.01
T1 (ms)	653 ± 65 (476–855)	668 ± 61 (535–855)	633 ± 66 (476–805)	0.002
T2 (ms)	36 ± 4 (26–49)	37 ± 4 (27–46)	35 ± 4 (26–49)	0.008
T1 ρ (ms)	45 ± 5 (30–60)	46 ± 5 (30–60)	45 ± 6 (32–55)	0.58

Values are in mean±SD (range)

BMI body mass index, PDFF Proton density fat fraction

P value compared between men and women.

Table 2 Sex-specific correlations of MRI parameters with age, BMI, visceral fat, and subcutaneous fat (Pearson correlation coefficient *r* (*P* value))

	Age (years)		BMI (kg/m ²)		Visceral fat (ml)		Subcutaneous fat (ml)	
	Women	Men	Women	Men	Women	Men	Women	Men
PDFF (%)	-0.02 (0.9)	-0.17 (0.2)	0.41 (<0.0001)	0.42 (0.001)	0.29 (0.008)	0.44 (<0.0001)	0.36 (0.001)	0.28 (0.026)
R2* (s ⁻¹)	0.33 (0.002)	0.04 (0.8)	0.18 (0.1)	0.07 (0.6)	0.1 (0.4)	0.08 (0.5)	0.31 (0.005)	0.01 (0.9)
T1 (ms)	-0.34 (0.002)	-0.24 (0.06)	0.02 (0.8)	0.31 (0.012)	-0.1 (0.4)	0.1 (0.4)	-0.02 (0.8)	0.15 (0.2)
T2 (ms)	-0.4 (<0.0001)	-0.14 (0.3)	-0.19 (0.08)	0.25 (0.05)	-0.31 (0.004)	0.04 (0.8)	-0.25 (0.02)	0.24 (0.6)
T1 ρ (ms)	0.01 (0.8)	0.27 (0.035)	-0.3 (0.006)	-0.15 (0.2)	-0.23 (0.04)	0 (0.9)	-0.28 (0.01)	-0.21 (0.1)

BMI body mass index, PDFF Proton density fat fraction

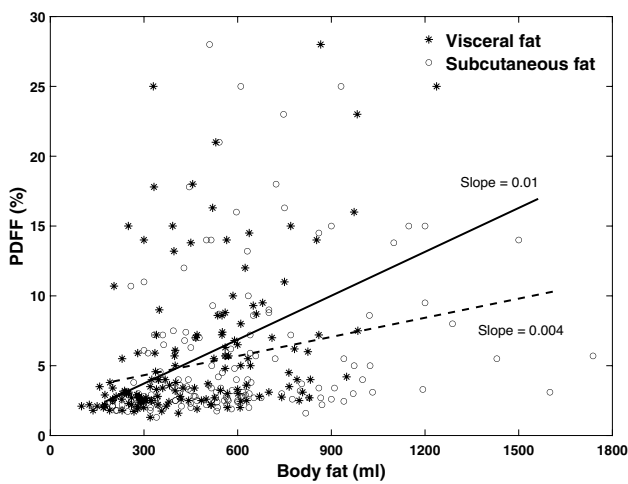


Fig. 2 Scatter plots show the correlations between liver proton density fat fraction (PDFF) and visceral fat and subcutaneous fat. The slope is the percent gain of liver fat per ml of body fat accretion

subcutaneous fat in women. All MRI parameters demonstrated sex difference except for T1ρ. PDFF and R2* were higher in men (both $P = 0.01$) while T1 and T2 were higher in women (both $P < 0.01$). Sex-stratified age, BMI, visceral and subcutaneous fat dependencies are presented in Table 2. PDFF was positively correlated with BMI and body fat but not to age in all adults. All parametric mapping parameters demonstrated sex-specific age and body fat dependence. R2* was positively but T1 and T2 were negatively associated with age in women (all $P < 0.01$). These relationships were not observed in men while T1ρ was positively related to age in men ($P < 0.05$). In co-variate adjusted linear regression analysis, only the visceral fat remained correlated to liver fat ($P < 0.0001$), not the subcutaneous fat ($P = 0.052$). The slope of the scatter plot between visceral fat and liver fat was greater than that of the subcutaneous fat in relationship to liver fat (Figure 2). Each 100 ml greater visceral or subcutaneous fat was associated with 1% or 0.4%, respectively, greater liver fat.

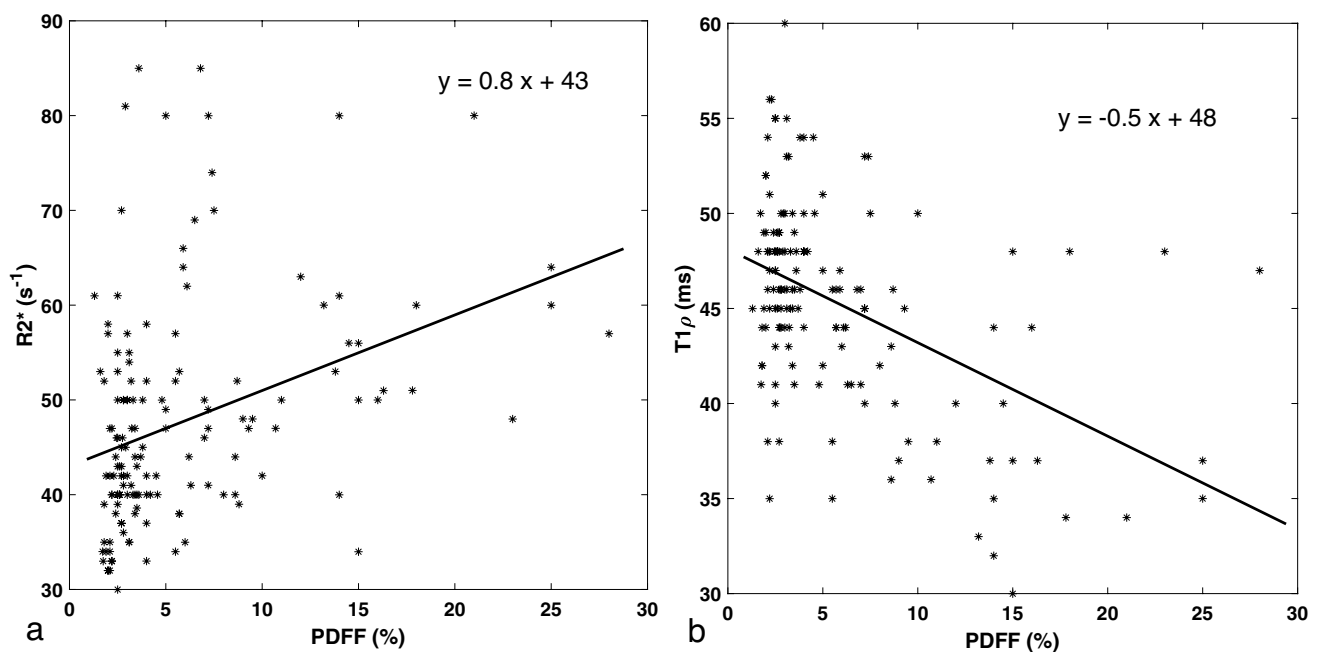


Fig. 3 Scatter plots show the correlations between liver proton density fat fraction (PDFF) and **a** R2* **b** T1ρ

Table 3 Matrix for the correlations between multiparametric MRI parameters (adjusted beta (P value))

	R2* (s ⁻¹)	T1 (ms)	T2 (ms)	T1ρ (ms)
PDFF (%)	0.14 (<0.0001)	0 (0.9)	- 0.01 (0.9)	- 0.36 (<0.0001)
R2* (s ⁻¹)		- 0.1 (<0.0001)	- 2 (<0.0001)	- 0.57 (0.001)
T1 (ms)			9 (<0.0001)	0.6 (0.5)
T2 (ms)				0.09 (0.11)

Correlation was age, sex, and BMI adjusted, PDFF Proton density fat fraction

No notable PDFF dependencies of T1 and T2 were observed. $R2^*$ was positively and T1 ρ was negatively associated with PDFF (both $P < 0.0001$, Figure 3a, b). $R2^*$ showed inverse correlations with T1, T2, and T1 ρ (all $P \leq 0.001$). T1 and T2 were directly correlated ($P < 0.0001$). There were no associations of PDFF with T1 and T2. T1 ρ was not correlated with T1 or T2. A correlation matrix with adjusted beta and P values for all parameters is given in Table 3.

Discussion

The present study analyzed the associations of each relaxometry index and PDFF with sex specific ageing and anthropometric variables in adult livers of individuals without clinical hepatic disease. MR relaxometry measures remain controversial in the evaluation of liver fibrosis. The excessive deposition of collagen and expansion of extracellular matrix in the fibrotic tissue does not necessarily lead to prolonged T1, T2, and T1 ρ when concomitant with fat and iron depositions, which are common in chronic liver disease [7–10]. Fat possesses a much shorter T1 than water, and iron reduces all tissue relaxation times. Furthermore, technical limitations in the acquisition and reconstruction of relaxometry maps should be considered when using MRI-derived biomarkers [5, 6]. Given the extensive overlaps in the range of relaxation times across different stages of hepatic fibrosis in the published literature, it is very relevant to understand the distributions and inter-relationships among these MRI parameters in the liver of apparently healthy individuals before the onset of clinical hepatic disease.

Our cohort was comprised of volunteers with a broad range of age and BMI selected from the local community. None of the study participants, including those with high PDFF values had prior diagnosis of fatty liver disease. We found that most of MRI parameters demonstrated sex-specific distribution and age and body fat dependencies. The disparities could be explained by physiological differences in parameters such as serum ferritin and hemoglobin levels. Kühn et al reported sex-specific patterns between PDFF and age in a population-based study of 2,561 participants [11]. The same study also found higher $R2^*$ in men than in women and age association of $R2^*$ in women. Schwenzer et al assessed liver, spleen, and pancreas T2* decay in a healthy cohort ($N = 129$) [12]. In their study both among women and men, significant correlations between age and T2* values were found, and could be attributed to age-related increase in serum ferritin.

Age and sex were not related to liver T1 in the UK biobank data which included a low-risk population of 1,037 individuals recruited from the community (BMI < 25 kg/m² and PDFF < 5%) [13]. In the study conducted

by Ghavamian et al in 60 healthy volunteers, sex also had no impact on liver T1 [14]. However, both T1 and T2 were different between sex and demonstrated age dependency in women in our study. Liver T1 ρ was previously reported to be negatively associated with age in normal female livers but not in men, and was found to be independent of BMI [15]. Conversely, BMI is related to PDFF in adults as determined in the current study and previously reported in other studies [24]. Moreover, we found that liver fat is more related to visceral than subcutaneous fat. This might explain why men demonstrated greater liver fat than that in women given both had similar BMI in our current findings.

Elevated T1 has been observed consistently in patients with hepatic fibrosis. The presence of steatosis was associated with a higher risk of fibrosis progression [16]. Co-occurrence of liver fat and fibrosis complicates the behavior of relaxation times. Fat has a much shorter T1 than that of water, so it is reasonable to expect that tissue T1 be reduced in the presence of fat. However, in using the MOLLI sequence, T1 is artificially elevated when fat and water coexist [5, 17]. When including the UK biobank whole cohort ($N = 2816$), weak but significant correlation between hepatic T1 value and PDFF was reported, and the authors suggested that the MOLLI acquisition was the culprit [13]. Our MOLLI T1 mapping method was optimized to reduce the impact of fat. Although no association was discovered between T1 and PDFF in our study, other factors such as sample size and field strength should be considered when comparing our findings to those of other studies.

Preclinical studies have demonstrated strong and positive correlations of T1 ρ to liver collagen content and fibrosis stage [18, 19]. The usefulness of T1 ρ in differentiating fibrotic from normal human liver tissue has also been described [20, 21]. While T1 ρ seemed to be unaffected by steatosis in clinical studies [21, 22], the effect of fat has been postulated to shorten T1 ρ in a well-controlled experimental setting [20, 23]. Interestingly, we have observed a negative association between PDFF and T1 ρ , which highlights fat as a potential confounder when utilizing T1 ρ to detect liver fibrosis. In accordance with several previous findings, PDFF was also directly linked to $R2^*$ in our study [13, 24, 25]. In contrast, T2 values were not related to steatosis in a murine model and other studies also showed no difference between fatty and normal livers in humans [26, 27]. T2 appears insensitive to PDFF as suggested by the data presented here. Fat T2 is substantially greater than in normal liver parenchyma or muscle. In this regard, skeletal muscle with fatty replacement exhibits elevated T2 relaxation times [28]. The mechanism by which T2 is unaffected by hepatic fat content requires further investigation.

There are several limitations in our study. The nature of the study precluded the use of biopsy as the reference standard. Blood was not collected for metabolic syndrome

assessment. Only 6 participants with diabetes but exclusion of these studies did not change the results. Status of liver disease was based on self-report. We modeled the association between body fat and PDFF by linear regression. However, the relationship could be convoluted and exploration of best fit is beyond the scope of current work. All imaging data used in this study was acquired on a single 3 T scanner. In addition, liver imaging methods that were employed in the study can theoretically affect the reported associations. For example, the protocol for T1 mapping was set to minimize the influence of fat [6]. This is crucial for the purpose of utilizing T1 to evaluate fibrosis to tease apart the contribution of fat. Fat saturation techniques could have also been used but they are not commonly employed in mapping sequences. Little is known about the association of relaxometry times and fat in normal livers and their behavior in the presence of iron and fibrosis. More recently, sub-clinical liver imaging has been employed to gain insight on pathologic processes involving other organ systems such as the cardiovascular system and musculoskeletal apparatus [29, 30]. Most proteins involved in the control of innate immunity, coagulation and inflammation are produced in the liver placing this organ at the center of diverse pathologic processes influencing homeostasis across the entire human body. The data obtained in this study should provide support for future sub-clinical and clinical studies using 3 T hepatic mapping.

Conclusions

Sex plays an important role in the body fat distribution as well as the normal ranges of hepatic $R2^*$, T1, and T2 values. Visceral fat plays an essential role in the elevated liver fat. Multiparametric MRI measures have sex-specific age and body fat dependencies. Relaxometry hepatic mapping indices are related to PDFF. Indeed, significant associations between PDFF and both $R2^*$ and T1 ρ but not with T1 or T2 were found. When using MRI measures for liver disease evaluation, interactions among hepatic mapping parameters should be considered.

Funding This study was supported by Canon Medical Systems Corporation.

Declarations

Conflict of interest Chia-Ying Liu, Bruno Triaire, and Yoshimori Kasai are Canon employees. Joao Lima has received research support from Canon medical systems. All other authors declare that they have no conflicts of interest.

References


1. Thomaidis-Brears HB, Lepe R, Banerjee R and Duncker C. Multiparametric MR mapping in clinical decision-making for diffuse liver disease. *Abdom Radiol (NY)*. 2020;45:3507-3522.
2. Arieira C, Monteiro S, Xavier S, Dias de Castro F, Magalhaes J, Marinho C, Pinto R, Costa W, Pinto Correia J and Cotter J. Transient elastography: should XL probe be used in all overweight patients? *Scand J Gastroenterol*. 2019;54:1022-1026.
3. Lee YS, Yoo YJ, Jung YK, Kim JH, Seo YS, Yim HJ, Kim IH, Lee SY, Kim BH, Kim JW, Lee CH, Yeon JE, Kwon SY, Um SH and Byun KS. Multiparametric MR Is a Valuable Modality for Evaluating Disease Severity of Nonalcoholic Fatty Liver Disease. *Clin Transl Gastroenterol*. 2020;11:e00157.
4. Marti-Aguado D, Rodriguez-Ortega A, Alberich-Bayarri A and Marti-Bonmati L. Magnetic Resonance imaging analysis of liver fibrosis and inflammation: overwhelming gray zones restrict clinical use. *Abdom Radiol (NY)*. 2020;45:3557-3568.
5. Liu CY, Noda C, Ambale-Venkatesh B, Kassai Y, Bluemke D and Lima JAC. Evaluation of liver T1 using MOLLI gradient echo readout under the influence of fat. *Magn Reson Imaging*. 2022;85:57-63.
6. Mozes FE, Tunnicliffe EM, Moolla A, Marjot T, Levick CK, Pavlides M and Robson MD. Mapping tissue water T1 in the liver using the MOLLI T1 method in the presence of fat, iron and B0 inhomogeneity. *NMR Biomed*. 2019;32:e4030.
7. Tunnicliffe EM, Banerjee R, Pavlides M, Neubauer S and Robson MD. A model for hepatic fibrosis: the competing effects of cell loss and iron on shortened modified Look-Locker inversion recovery T1 (shMOLLI-T1) in the liver. *J Magn Reson Imaging*. 2017;45:450-462.
8. Cassinotto C, Feldis M, Vergniol J, Mouries A, Cochet H, Lapuyade B, Hocquelet A, Juanola E, Foucher J, Laurent F and De Ledinghen V. MR relaxometry in chronic liver diseases: Comparison of T1 mapping, T2 mapping, and diffusion-weighted imaging for assessing cirrhosis diagnosis and severity. *Eur J Radiol*. 2015;84:1459-1465.
9. Hoad CL, Palaniyappan N, Kaye P, Chernova Y, James MW, Costigan C, Austin A, Marciani L, Gowland PA, Guha IN, Francis ST and Aithal GP. A study of T(1) relaxation time as a measure of liver fibrosis and the influence of confounding histological factors. *NMR Biomed*. 2015;28:706-14.
10. Takayama Y, Nishie A, Asayama Y, Ushijima Y, Okamoto D, Fujita N, Morita K, Shirabe K, Kotoh K, Kubo Y, Okuaki T and Honda H. T1 rho Relaxation of the liver: A potential biomarker of liver function. *J Magn Reson Imaging*. 2015;42:188-95.
11. Kuhn JP, Meffert P, Heske C, Kromrey ML, Schmidt CO, Mensel B, Volzke H, Lerch MM, Hernando D, Mayerle J and Reeder SB. Prevalence of Fatty Liver Disease and Hepatic Iron Overload in a Northeastern German Population by Using Quantitative MR Imaging. *Radiology*. 2017;284:706-716.
12. Schwenzer NF, Machann J, Haap MM, Martirosian P, Schraml C, Liebig G, Stefan N, Haring HU, Claussen CD, Fritzsche A and Schick F. T2* relaxometry in liver, pancreas, and spleen in a healthy cohort of one hundred twenty-nine subjects-correlation with age, gender, and serum ferritin. *Invest Radiol*. 2008;43:854-60.
13. Mojtahed A, Kelly CJ, Herlihy AH, Kin S, Wilman HR, McKay A, Kelly M, Milanese M, Neubauer S, Thomas EL, Bell JD, Banerjee R and Harisinghani M. Reference range of liver corrected T1 values in a population at low risk for fatty liver disease—a UK Biobank sub-study, with an appendix of interesting cases. *Abdom Radiol (NY)*. 2019;44:72-84.
14. Ghavamian A, Liu C, Kang B, Yuan X, Wang X, Gao L and Zhao X. Liver T1 relaxation time of the 'normal liver' in healthy

- Asians: measurement with MOLLI and B1-corrected VFA methods at 3T. *Br J Radiol.* 2022;20211008.
15. Wang YXJ, Deng M, Lin J, Kwok AWL, Liu EKW and Chen W. Age- and Gender-Associated Liver Physiological T1rho Dynamics Demonstrated with a Clinically Applicable Single-Breathhold Acquisition. *SLAS Technol.* 2018;23:179-187.
 16. McPherson S, Hardy T, Henderson E, Burt AD, Day CP and Anstee QM. Evidence of NAFLD progression from steatosis to fibrosing-steatohepatitis using paired biopsies: implications for prognosis and clinical management. *J Hepatol.* 2015;62:1148-55.
 17. Mozes FE, Tunnicliffe EM, Pavlides M and Robson MD. Influence of fat on liver T1 measurements using modified Look-Locker inversion recovery (MOLLI) methods at 3T. *J Magn Reson Imaging.* 2016;44:105-11.
 18. Hu G, Zhang X, Liang W, Zhong X, Chan Q, Lin X, Lin T, Li Y and Quan X. Assessment of liver fibrosis in rats by MRI with apparent diffusion coefficient and T1 relaxation time in the rotating frame. *J Magn Reson Imaging.* 2016;43:1082-9.
 19. Zhao F, Zhou N, Wang JL, Zhou H, Zou LQ, Zhong WX, He J, Zheng CJ, Yan SX and Wang YXJ. Collagen deposition in the liver is strongly and positively associated with T1rho elongation while fat deposition is associated with T1rho shortening: an experimental study of methionine and choline-deficient (MCD) diet rat model. *Quant Imaging Med Surg.* 2020;10:2307-2321.
 20. Allkemper T, Sagmeister F, Cicinnati V, Beckebaum S, Kooijman H, Kanthak C, Stehling C and Heindel W. Evaluation of fibrotic liver disease with whole-liver T1rho MR imaging: a feasibility study at 1.5 T. *Radiology.* 2014;271:408-15.
 21. Xie S, Li Q, Cheng Y, Zhang Y, Zhuo Z, Zhao G and Shen W. Impact of Liver Fibrosis and Fatty Liver on T1rho Measurements: A Prospective Study. *Korean J Radiol.* 2017;18:898-905.
 22. Qian Y, Hou J, Jiang B, Wong VW, Lee J, Chan Q, Wang Y, Chu WC and Chen W. Characterization and correction of the effects of hepatic iron on T1rho relaxation in the liver at 3.0T. *Magn Reson Med.* 2022;88(4):1828–1839.
 23. Zhao F, Zhou N, Wang X, Wang JL, Zhong WX, Deng M, Zheng CJ, He J, Yan SX and Wang YXJ. T1rho shortening effect of fat in liver steatosis after fat suppression: approximate estimation in a methionine and choline-deficient (MCD) diet rat model. *Quant Imaging Med Surg.* 2021;11:870-875.
 24. Karlsson M, Ekstedt M, Dahlstrom N, Forsgren MF, Ignatova S, Noren B, Dahlqvist Leinhard O, Kechagias S and Lundberg P. Liver R2* is affected by both iron and fat: A dual biopsy-validated study of chronic liver disease. *J Magn Reson Imaging.* 2019;50:325-333.
 25. Mamidipalli A, Hamilton G, Manning P, Hong CW, Park CC, Wolfson T, Hooker J, Heba E, Schlein A, Gamst A, Durelle J, Paiz M, Middleton MS, Schwimmer JB and Sirlin CB. Cross-sectional correlation between hepatic R2* and proton density fat fraction (PDFF) in children with hepatic steatosis. *J Magn Reson Imaging.* 2018;47:418-424.
 26. Erden A, Kuru Oz D, Peker E, Kul M, Ozalp Ates FS, Erden I and Idilman R. MRI quantification techniques in fatty liver: the diagnostic performance of hepatic T1, T2, and stiffness measurements in relation to the proton density fat fraction. *Diagn Interv Radiol.* 2021;27:7-14.
 27. Wang X, Hu Y, Lu X, Cai Y and Shu J. Quantitative T2 mapping of rats with chronic hepatitis. *Exp Ther Med.* 2021;21:225.
 28. Liu CY, Yao J, Kovacs WC, Shrader JA, Joe G, Ouwerkerk R, Mankodi AK, Gahl WA, Summers RM and Carrillo N. Skeletal Muscle Magnetic Resonance Biomarkers in GNE Myopathy. *Neurology.* 2021;96:e798-e808.
 29. Arora A, Rajesh S, Bansal K, Sureka B, Patidar Y, Thapar S and Mukund A. Cirrhosis-related musculoskeletal disease: radiological review. *Br J Radiol.* 2016;89:20150450.
 30. Ostovaneh MR, Ambale-Venkatesh B, Fuji T, Bakhshi H, Shah R, Murthy VL, Tracy RP, Guallar E, Wu CO, Bluemke DA and Lima JAC. Association of Liver Fibrosis With Cardiovascular Diseases in the General Population: The Multi-Ethnic Study of Atherosclerosis (MESA). *Circ Cardiovasc Imaging.* 2018;11:e007241.

Publisher's Note Springer Nature remains neutral with regard to jurisdictional claims in published maps and institutional affiliations.

Springer Nature or its licensor (e.g. a society or other partner) holds exclusive rights to this article under a publishing agreement with the author(s) or other rightsholder(s); author self-archiving of the accepted manuscript version of this article is solely governed by the terms of such publishing agreement and applicable law.

Authors and Affiliations

Chia-Ying Liu¹  · Chikara Noda² · Rob J van der Geest³ · Bruno Triaire¹ · Yoshimori Kassai¹ · David A. Bluemke⁴ · João A. C. Lima²

✉ Chia-Ying Liu
cliu@mru.medical.canon

¹ Canon Medical Systems Corporation, Otawara, Japan

² Division of Cardiology, Johns Hopkins University School of Medicine, Baltimore, MD, USA

³ Department of Radiology, Leiden University Medical Center, Leiden, The Netherlands

⁴ Department of Radiology, University of Wisconsin, Madison, WI, USA